Nanochem Res 3(1): 62-78, Winter and Spring 2018

REVIEW PAPER

Carbon Dioxide Capture on Metal-organic Frameworks with Amide-decorated Pores

Sima Kazemi and Vahid Safarifard*

Department of Chemistry, Iran University of Science and Technology, Tehran, Iran

ARTICLE INFO

Article History:
Received 26 November 2017
Accepted 19 January 2018
Published 1 March 2018

Keywords:
Amide
CO_2 Capture
Metal-Organic Frameworks

ABSTRACT

CO_2 is the main greenhouse gas emitted from the combustion of fossil fuels and is considered a threat in the context of global warming. Carbon capture and storage (CCS) schemes embody a group of technologies for the capture of CO_2 from power plants, followed by compression, transport, and permanent storage. Key advances in recent years include the further development of new types of porous materials with high affinity and selectivity toward CO_2 for optimizing the energy penalty of capture. In this regard, microporous metal-organic frameworks (MOFs) represent an opportunity to create next-generation materials that are optimized for real-world applications in CO_2 capture. MOFs have great potential in CCS because they can store greater amounts of CO_2 than other classes of porous materials, and their chemically-adjustable organic and inorganic moieties can be carefully pre-designed to be suitable for molecular recognition of CO_2. Taking into account the nature of physisorption and inherent polarity of CO_2 molecules, addressing materials with both a large surface area and polar pores for strong CO_2 binding affinity is an effective method. Decorating the pores of MOFs with some specific functional groups by directly using functionalized organic linkers or postsynthetic modification, that have high binding affinity to CO_2 molecules, is among the most promising strategies has been pursued to achieve high-performance CO_2 uptake. This review highlights the literature reported on MOFs with amide-decorated pores for CO_2 capture, showing the effects of amide groups on uptake capacity, selectivity and adsorption enthalpies of CO_2.

How to cite this article
Kazemi S, Safarifard V. Carbon Dioxide Capture on Metal-organic Frameworks with Amide-decorated Pores. Nanochem Res, 2018; 3(1): 62-78. DOI: 10.22036/ncr.2018.01.007

INTRODUCTION

Economical and efficient carbon capture and sequestration (CCS) technologies has been attracting tremendous attention due to the escalated global warming [1-3]. A class of crystalline porous materials, metal-organic frameworks (MOFs) or porous coordination polymers (PCPs) that assembled by organic linkers and inorganic nodes (metal ions or metal-containing clusters), is of great promise for their potential use in the strategic storage and separation of hydrogen, methane, and carbon dioxide in clean-energy applications [4-10]. High surface area, large total pore volume and high adsorption enthalpy involving host-guest interactions are all crucial for high-performance CO_2 storage MOF materials [11]. Therefore, MOF research is currently addressing two issues: (i) increasing CO_2 uptake by generation of MOFs with even higher surface areas and larger pore volumes by the use of larger bridging ligands or highly connected secondary building units (SBUs) [12-15] and (ii) increasing the selectivity of MOFs through enhancement of the adsorption enthalpies for CO_2 through decoration of the materials [16-22]. Until now, several strategies have been pursued to achieve the latter goal, such as narrowing the pore

* Corresponding Author Email: *vsafarifard@iust.ac.ir*

size by interpenetration [23-25], tuning of the pore surface charge through variation of the metal cation [26], introducing an alkylamine functionality [27] or water molecules [28] onto the coordinatively unsaturated metal center and decorating MOFs with some specific functional groups (-NH_2, -NO_2, -OH, etc.) that have high binding affinity to CO_2 molecules by postsynthetic modification or directly using functionalized organic linkers [29-34].

The incorporation of pendant amide (-CONH-) groups into MOFs is regarded as a promising approach to enhance CO_2 uptake due to the formation of hydrogen bonds with amides serving as both hydrogen bond acceptors (*via* C=O) and donors (*via* N-H) [35-41]. Amide groups have the same positive effect on adsorption of CO_2 like the widely reported amine (-NH_2) groups by facilitating dipole-quadrupole interactions [20]. However, these two analogous functional groups have some different structural and chemical characteristics. The amide group usually does not coordinate with metal ions and keeps open status in process of constructing MOFs, although it may increase the structural flexibility of MOFs because of its customary position in the main carbon skeleton of the organic ligands. While, the amine group may coordinate with metal ions and loses its function to interact with CO_2 when the amine-functionalized organic ligands are employed in synthesizing MOFs. On the other hand, the amine group is not located on the main carbon skeleton of the organic ligands and has no apparent influence on the rigidity or flexibility of the MOFs' structures [42]. A series of amide-functionalized MOFs have been synthesized and shown to exhibit high CO_2 uptakes and selectivity (Table 1). However, the incorporation of this functional group generally improves capacity only modestly at low pressures. Likewise, computational studies attribute this to the specific binding and formation of hydrogen bonds between adsorbed CO_2 molecules and free amide groups thus enhancing adsorption affinity and selectivity for CO_2. Several review papers have been published about the MOFs with large CO_2 storage capacity and high selectivity [43-46], but the effects of amide groups in CCS performance of MOFs with amide-decorated pores was not mentioned. This issue is presented in this review.

First evidence

In 2011, Bai and Zaworotko [37] reported how amide groups inside the pores of a Cu-based MOF, $[Cu_{24}(TPBTM^{6-})_8(H_2O)_{24}]$ (Cu-TPBTM), can result in a larger CO_2 uptake, enhanced heat of adsorption, and a higher selectivity toward CO_2/N_2 in comparison with an analogous MOF with alkyne groups. Solvothermal reaction of $Cu(NO_3)_2.3H_2O$ with flexible C_3-symmetric hexacarboxylate ligand of TPBTM (TPBTM = N,N',N"-tris(isophthalyl)-1,3,5- benzenetricarboxamide) with

Table 1: A series of amide-functionalized MOFs have been synthesized and shown to exhibit CO_2 uptakes

Chemical formula	Common name	BET (m^2g^{-1})	Capacity (wt %)	pressure (bar)	temp (K)	- Q_{st} $kJmol^{-1}$	*Ref.*
$[Cu_2(H_2O)_2BDPO]$	NOTT-125	2447	40.1 [93.3]	1 [20]	273	25.4	[36]
$[Cu_{24}(TPBTM_{6-})_8(H_2O)_{24}]$	Cu-TPBTM	3160	103.5	20	298	26.3	[37]
$[Cu(pia)_2(SiF_6)](EtOH)_2(H_2O)_{12}$	UTSA-48	285	5.5	1	296	30	[42]
$[Cu_3(BTB^{6-})]_n$	Cu-BTB	3288	157	20	273	-	[50]
$Cu_3L_2(H_2O)_5]$	NJU-Bai3	2690	27.3 [97.7]	1 [20]	273	-	[55]
$[Cu_2PDAI(H_2O)]$	PCN-124	1372	28.6	1	273	26.3	[59]
$[Zn_4(bdc)_4(bpda)_4]\cdot$ 5DMF·$3H_2O$	Zn-bpda	331	15.2	35	298	30.2	[61]
$[Cu_2(TCMBT)(bpp)(\mu_3\text{-}OH)]\cdot 6H_2O$	Cu.TCMBT	808.5	25.5	20	298	26.7	[62]
$[Cu_2(BDPT^{4-})(H_2O)_2]$	HNUST-1	1400	30.7	1	273	22.3	[65]
$[Cu_2BDPO(H_2O)_4]$	HNUST-3	2412	98.9	20	273	24.8	[67]
$[CuL_2(NO_3)_2\cdot$o-xylene·DMF$]_n$	$1\supset NO_3^-$		16.5	1	195	-	[73]
$[Mn_2(2,6\text{-}ndc)_2(bpda)_2]\cdot$5DMF	Mn-bpda	372	26.9	35	298	29.6	[74]
$[Zn_2(oba)_2(bpta)]\cdot(DMF)_3$	TMU-22	680	31.7	1	203	26	[76]
$[Zn_2(oba)_2(bpfb)]\cdot(DMF)_5$	TMU-23	0	31.7	1	203	-	[76]
$[Zn_2(oba)_2(bpfn)]\cdot(DMF)_2$	TMU-24	0	27.7	1	203	24	[76]
$[Zr_6(\mu_3\text{-}O)_4(\mu_3\text{-}OH)_4(\text{-}OH)_4(\text{-}OH_2)_4(TBAPy)_2]$	SALI-F3G	890	7.3	1	273	27	[77]
-	SALI-DAP	1225	10.1	1	273	28	[77]
$[Cu_2(PDAD)(H_2O)]_n$	PCN-124-stu	2153	31.4	1	273	26	[79]
-	MFM-136	1634	63	20	273	25.6	[80]

amide groups afforded a high yield of octahedron shaped crystals of Cu-TPBTM. This MOF exhibits the same topology as the prototypical *rht*-type MOF [47] and other isoreticular MOFs such as the PCN-61 series [48] and NOTT-112 [49] (Fig. 1a). The N_2 adsorption for Cu-TPBTM at 77 K exhibited a reversible type-I isotherm with BET surface area of ~3160 $m^2 g^{-1}$, which is close to PCN-61 (~3000 $m^2 g^{-1}$) and smaller than those reported for PCN-68 (~5109 $m^2 g^{-1}$) [48]. The effect of the amide groups upon CO_2 uptake on Cu-TPBTM is compared to its analogue PCN-61, which possesses the same pore sizes, surface area, and number of open Cu^{II} sites, where the only difference between Cu-TPBTM and PCN-61 is the substitution of the acetylene moiety in PCN-61 with an amide moiety (Fig. 1b). Interestingly, Cu-TPBTM exhibits a stronger binding affinity for CO_2 than PCN-6. CO_2 adsorption capacity of Cu-TPBTM is ca. 23.53 mmol g^{-1} at 298 K and 20 bar, with a corresponding isosteric heat of adsorption of - 26.3 kJ/mol. These results are higher than PCN-66 (21.5 mmol g^{-1}; -22 kJ/mol) and PCN-68 (22.1 mmol g^{-1}; -21.2 kJ/mol), although the latter has larger surface areas (Fig. 1c, d). Moreover, better selectivity for CO_2/N_2 separation has been achieved at 298 K for Cu-TPBTM (~22 at 1 bar and 33 at 20 bar) compared to PCN-61 (15 at 1 bar and 22 at 20 bar). These suggest that polar -CONH- functionalities have a positive effect on adsorption of CO_2 by enhancing the initial slopes of CO_2 isotherms for Cu-TPBTM, resulting in greater Q_{st}, uptake, and selectivity.

In a similar study by the same group, nanosized triangular amide-bridging hexacarboxylate linkers of H_6BTB and H_6TATB have been used to expand isoreticular *rht*-type MOFs of $[Cu_3(BTB^{6-})]_n$ (Cu-BTB) and $[Cu_3(TATB^{6-})]_n$ (Cu-TATB) [50] (Fig. 2a). Cu-BTB and Cu-TATB exhibit a high apparent BET surface area of 3288 and 3360 $m^2 g^{-1}$, respectively, which is slightly higher than that of Cu-TPBTM. Both materials display uncommon pseudo type IV isotherms with stepwise adsorption behavior and a noticeable hysteresis, which is characteristic

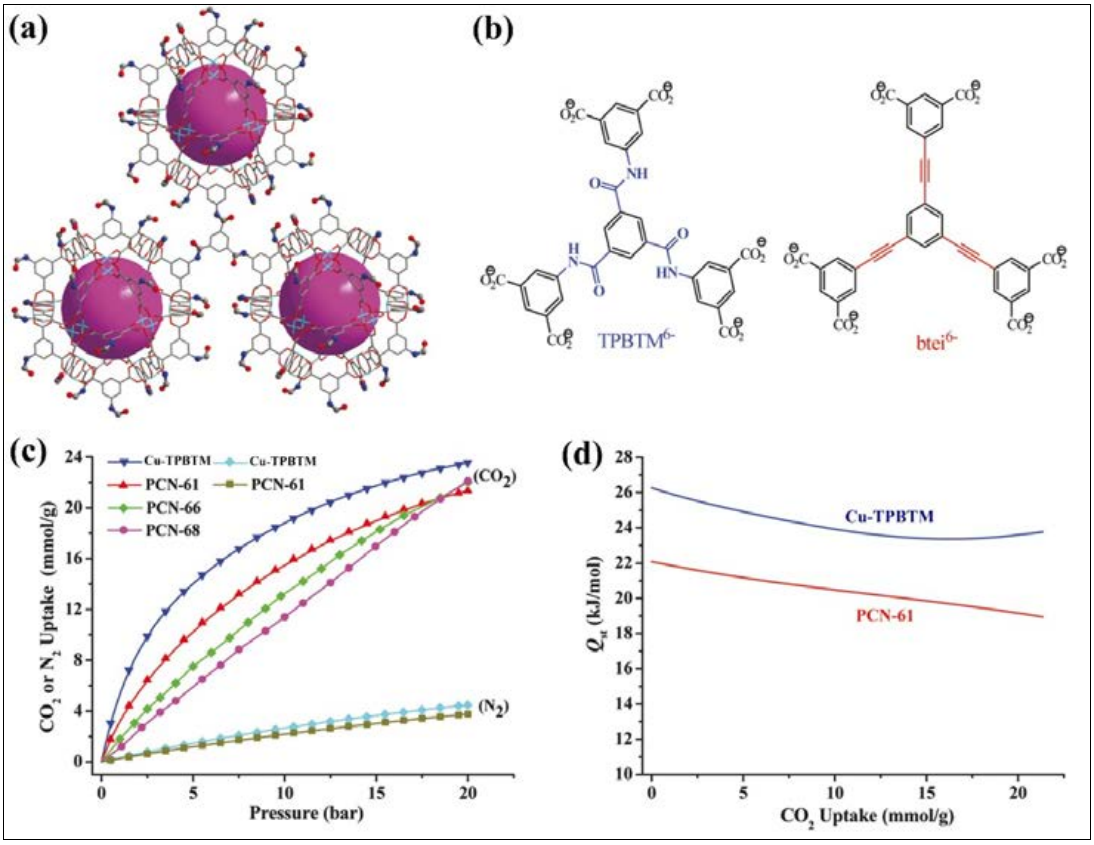

Fig. 1: (a) Portion of the structure of the (3, 24)-connected *rht*-type framework of Cu-TPBTM showing surface decoration by amide groups. Cu, blue-green; C, gray; O, red; N, blue. (b) Bridging ligands of $TPBTM^{6-}$ and $btei^{6-}$ for Cu-TPBTM and PCN-61, respectively. (c) High-pressure gravimetric excess CO_2 and N_2 sorption isotherms of Cu-TPBTM and the PCN-6X series at 298 K. (d) Isosteric heats of CO_2 adsorption for Cu-TPBTM and PCN-61. Adapted from Ref. [37].

of flexible MOFs with hierarchically-assembled mesopores. High-pressure gravimetric CO_2 adsorption isotherms show that compared to the parent Cu-TPBTM MOF, the CO_2 sorption isotherm of expanded framework Cu-BTB demonstrates a type-IV-like profile with a marked gate-opening process with an exceptionally high unsaturation excess CO_2 uptake of 111 wt% at 298 K. This CO_2 storage capacity is just lower than that of MOF-177 (123.2 wt%) [12] and MOF-205 (114.4 wt%) [15], but far greater than that of any other high surface area MOFs reported such as MOF-210 (70.4 wt%) [15] and NU-100 (95 wt%) [51] under the same conditions. Interestingly, in sharp contrast to CO_2, Cu-BTB can only absorb limited amounts of CH_4 (13 wt%) and N_2 (11 wt%) at 273 K and 20 bar, representing the CO_2/CH_4 and CO_2/N_2 selectivity of 8.6 and 34.3, respectively, which are much higher than the corresponding value of MOF-177 (4.4 and 17.5) [52] and most other MOF materials [53].

The introduction of N-heteroaryl moieties into MOFs may generally lead to the improvement of their CO_2 storage abilities which was confirmed by theoretical studies [54]. However, in the case of Cu-TATB, it was almost useless, and Cu-TATB had almost the same gas sorption behavior as Cu-BTB, despite that the surface is decorated by nitrogen containing triazine rings. Moreover, grand canonical Monte Carlo (GCMC) and first-principles calculations have been performed to further probe the advantages of amide groups upon CO_2 adsorption at the molecular level, which demonstrated that CO_2 molecules prefer to locate at both the open Cu(II) metal sites and amide groups within the Cu-BTB framework. More interestingly, the CO_2 binding energy of the carbonyl site (C=O) is up to -9.24 kJ mol^{-1} and is very comparable with that of open Cu^{II} metal sites (-9.03 kJ mol^{-1}), and far from the amide site (-NH-) (-0.168 kJ mol^{-1}) (Fig. 2b). The reason for this difference could be attributed to the possibility that the carbonyl moiety can yield an enhanced lone pair polarization on the CO_2 molecule. These results verified that the amide groups within both structures act as strong interaction sites and play an important role in the high and selective CO_2 uptake.

In a follow-up study by the same group, an *agw*-type porous MOF with the inserted amide functional groups, $[Cu_3L_2(H_2O)_5]$ (NJU-Bai3), has been reported based upon a relatively small multidentate ligand, 5-(4-carboxybenzoylamino)-isophthalic acid (H_3L) (Fig. 3a) [55]. The overall structure of NJU-Bai3 is well packed by three types of cages with densely decorated amide units that are directly exposed to each individual cavity, in which, the bowl-like cage includes 12 amide groups (Fig. 3b), exhibited the BET surface area of 2690 m^2g^{-1}. The CO_2 uptake for NJU-Bai3 at 273 K and 1 bar reaches 6.21 mmol g^{-1}, which is substantially larger than that of UMCM-150 (4.68 mmol g^{-1}), which the latter has the same topology as the prototypical

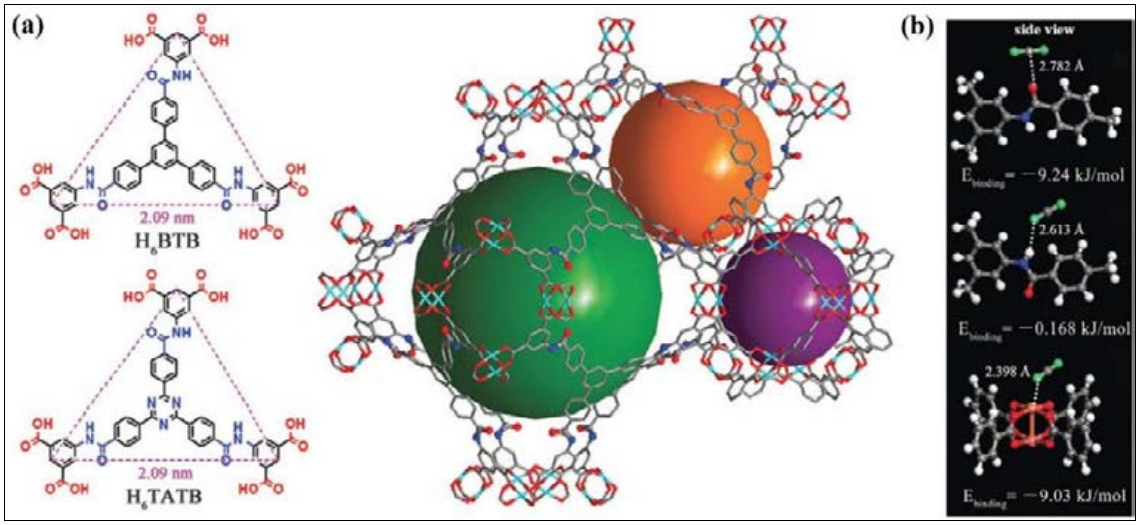

Fig. 2: (a) Nanosized amide-bridging ligands (H_6BTB and H_6TATB) and the 3D polyhedra packing in Cu-BTB. Cu, blue-green; C, gray; O, red; N, blue. (b) Preferential CO_2 adsorption sites and corresponding binding energies in Cu-BTB obtained from first-principles calculations. Adapted from Ref. [50].

agw-type framework but without amid-decorated pores [56]. Moreover, its high-pressure adsorption shows the unsaturation excess CO_2 uptake of 22.12 mmol g^{-1} at 273 K and 20 bar, which is among the highest values for porous MOFs (IRMOF-1: 19.0 mmol g^{-1}; IRMOF-3: 17.2 mmol g^{-1}; and MOF-177: 28.7 mmol g^{-1}). However, it is worthy of note that the corresponding N_2 and CH_4 uptake of NJU-Bai3 was only 3.96 mmol g^{-1} and 6.9 mmol g^{-1}, respectively.

Furthermore, the amide-functionalized NJU-Bai3 exhibits a strong binding affinity for CO_2 (36.5 kJ mol^{-1}) at zero coverage, which is significantly higher than that of its prototype, UMCM-150 (20.3 kJ mol^{-1}) [57]. Moreover, similar to the previous example, the authors used GCMC simulations to further investigate the positive effect of decorated amide groups on CO_2 uptake in NJU-Bai3, which clearly reveal that both Cu^{II} metal sites and the amide groups are the main adsorption sites of CO_2 molecules in the framework. Interestingly, in terms of adsorption selectivity of CO_2/N_2 (60.8) and CO_2/CH_4 (46.6), NJU-Bai3 represents one of the highest selectivities reported up to now for adsorbent materials, except that of the Co(II)-carborane coordination polymers (CO_2/N_2: 95 and CO_2/CH_4: 47), which has very low CO_2 uptake (1.7 mmol g^{-1}, 17 bar and 298 K) [58] (Fig. 3c). Therefore, NJU-Bai3 is one of the best examples of MOFs combining two interesting characters of high storage and high selectivity toward CO_2.

Zhou and coworkers reported a microporous multi-functional MOF PCN-124, which is constructed from Cu paddlewheel motifs and 5,5′-((pyridine-3,5-dicarbonyl)bis-(azanediyl)) diisophthalate (PDAI) ligand with two isophthalate and one pyridine groups connected through amide bonds [59]. PCN-124 possesses a self-interpenetrated (3, 36)-connected 3D structure with the BET surface areas are of 1372 $m^2 g^{-1}$ and moderate hydrostability, which is particularly relevant for potential applications in CO_2 capture technologies. Interestingly, the linearly arranged open metal sites and amide groups in its framework provide a favorable environment for CO_2 adsorption. CO_2 adsorption capacity of PCN-124 is 28.6 wt% at 273 K and 1 bar, with a corresponding heat of adsorption at

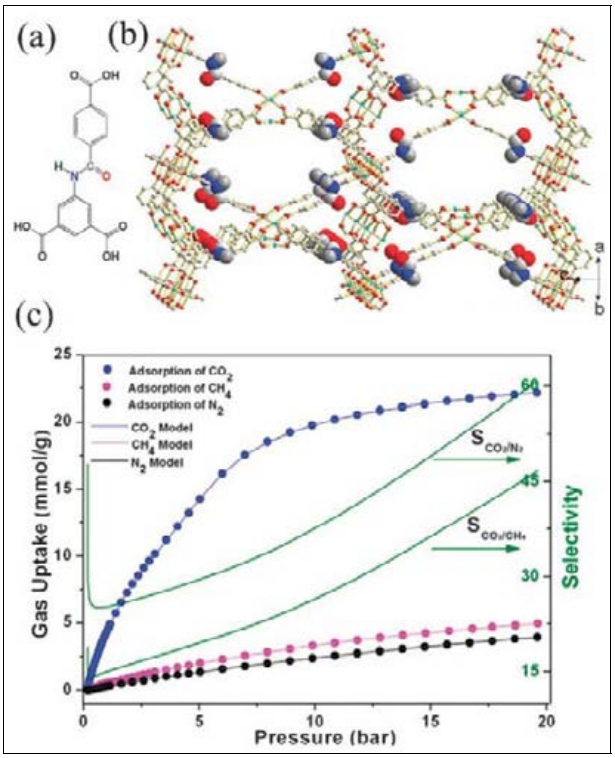

Fig. 3: (a) The organic building block of amide-functionalized H_3L. (b) The densely decorated amide groups in the pores from the crystal structure of NJU-Bai3. (c) High pressure gases adsorption isotherms and the dual-site Langmuir-Freundlich fit lines of CO_2, CH_4 and N_2 in NJU-Bai3 at 273 K. The green lines show the IAST predicted selectivity of CO_2 over N_2 and CH_4, respectively. Adapted from Ref. [55].

zero CO_2 loading of 26.3 kJ mol^{-1}. Interestingly, these results are higher than those for the isostructural MOF, PMOF-3, consisting of bridging ethynyl bonds instead of amide ones, despite higher N_2 adsorption of the latter.

In another report, a 3D microporous MOF with the formula of $[Cu(pia)_2(SiF_6)](EtOH)_2(H_2O)_{12}$ (UTSA-48; pia = N-(pyridin-4-yl) isonicotinamide) with functional -CONH- groups on the pore surfaces has been synthesized, and its CO_2 capture properties were compared to its isostructural amide-free MOFs, $[Cu(bipy)_2(SiF_6)]$ and $[Cu(bpe)_2(SiF_6)]$ [42]. The small pores and the functional amide groups within the activated UTSA-48 have enabled their strong interactions with CO_2, representing adsorption enthalpy of 30.0 kJ mol^{-1}, which is higher than the values of $[Cu(bipy)_2(SiF_6)]$ (27 kJ mol^{-1}) and $[Cu(bpe)_2(SiF_6)]$ (22 kJ mol^{-1}). Moreover, UTSA-48 exhibits CO_2/CH_4 separation with a Henry's Law selectivity of 20.7 at 273 K, which is higher than its isostructural non-functionalized MOFs [60], indicating that amide groups have the positive effect on adsorption of CO_2 by facilitating dipole-quadrupole interactions between -CONH- groups and CO_2 or NH···OCO hydrogen bonds.

Current developments

After the previous finding presented in the last section, researchers focused their efforts on studying the effect of amide on the CO_2 capture in MOFs. A unique spatial arrangement of amide groups for CO_2 adsorption was found in the open-ended channels of a zinc(II)-organic framework $[Zn_4(BDC)_4(bpda)_4]\cdot5DMF\cdot3H_2O$ (Zn-bpda; BDC = 1,4-benzyldicarboxylate, bpda = N,N′-bis(4-pyridinyl)-1,4-benzenedicarboxamide) [61]. Zn-bpda consists of 4^4-sql $[Zn_4(BDC)_4]$ sheets that are further pillared by a long amide-functionalized linker of bpda and forms a 3D porous framework with an α-Po $4^{12}\cdot6^3$ topology (Fig. 4a). The N_2

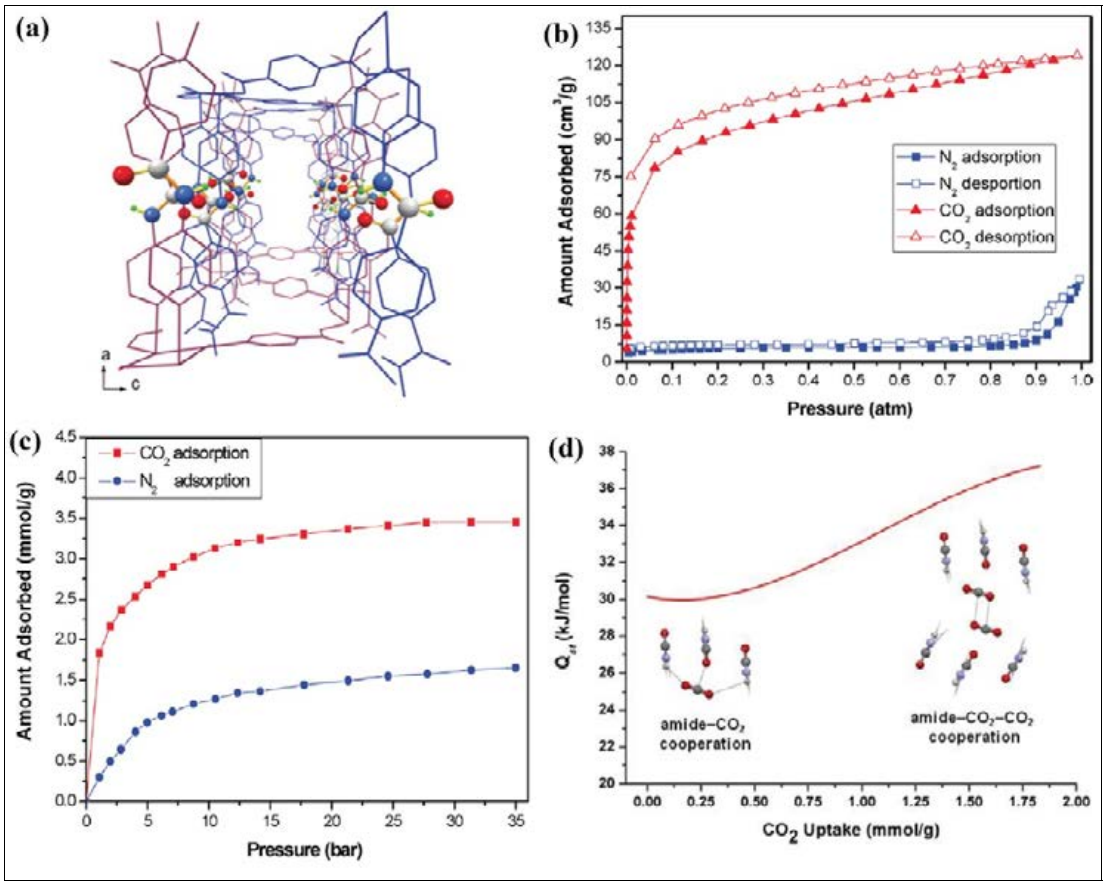

Fig. 4: (a) Spotlight of the larger channel opening showing a nearly unique arrangement of the unsheltered amide groups in Zn-bpda. Adsorption isotherms of N_2 and CO_2 measured at (b) 77 and 195 K and (c) 298 K and high pressure. (c) Isosteric heat (Q_{st}) of CO_2 adsorption. Adapted from Ref. [61].

adsorption isotherms of the MOF showed only a minor uptake at 77 K and 1 bar, which can be attributed to the framework contraction and a lack of appropriate intermolecular interactions at low temperature, where the CO_2 adsorption at 195 K exhibited a reversible type I isotherm, representing a BET surface area of 331 m^2 g^{-1} (Fig. 4b). Remarkably, the MOF takes up 3.45 mmol g^{-1} of CO_2 and 1.65 mmol g^{-1} of N_2 at 35 bar and 298 K, where displays a distinct selective adsorption capacity for CO_2 over N_2 at low pressure, (Fig. 4c). Interestingly, the amount of captured CO_2 molecules at 1 bar is nearly equivalent to the number of exposed amide groups of the framework. This fact, which was further approved by density functional theory (DFT) calculations, implies that the amide groups inside the framework are involved in efficient intermolecular interactions with the adsorbed CO_2 molecules at ambient pressure and temperature. Furthermore, due to the positive cooperative effect of the unsheltered amide groups on the adsorption of CO_2 molecules, the isosteric heat of CO_2 adsorption (Q_{st}) of Zn-bpda presented a strong binding affinity for CO_2 (30.2 kJ mol^{-1}), which exhibits a significant increase with increasing CO_2 uptake to 37.2 kJ mol^{-1}, depending on the adsorbed amount of CO_2 molecules (Fig. 4d).

Considering future practical applications, a good gas storage or separation material must be stable toward moisture. Bai and coworkers have presented an evolution approach for constructing a water stable pillar-layered porous MOF, $[Cu_2(TCMBT)(bpp)(\mu_3\text{-}OH)]\cdot 6H_2O$ (Cu-TCMBT), using amide-containing flexible N,N′,N″-tris(carboxymethyl)-1,3,5-benzenetricarboxamide (TCMBT) ligand [62]. Interestingly, Cu-TCMBT is quite stable in room temperature and boiling water for 2 months, as confirmed by PXRD patterns. The N_2 adsorption for activated Cu-TCMBT at 77 K exhibits a typical type I curve, with the BET surface area of 808.5 m^2 g^{-1}. In spite of possessing a relatively low BET surface area, the CO_2 uptake of Cu-TCMBT at 1 bar (44.8 cm^3 g^{-1}) outperforms those of most of the ZIF materials [30, 63]. Moreover, the adsorption enthalpies for CO_2, CH_4, and N_2 were calculated to be 26.7, 19.1 and 16.0 kJ mol^{-1}, respectively. The higher CO_2 adsorption enthalpy is mainly attributed to incorporated bridging amide groups along the small channels. Because of a much larger quadrupole moment of CO_2 (13.4×10^{-40} C m^2) than that of N_2 (4.7×10^{-40} C m^2) and CH_4 (nonpolar) [64], the large dipole moment of the bridging amide groups along the small channels facilitated the dipole-quadrupole interactions with CO_2, leading to the selectivity of CO_2 over CH_4 and N_2.

In 2013, Zheng *et al.* reported an expanded microporous NbO-type MOF formulated as $[Cu_2(BDPT^{4-})(H_2O)_2]$ (HNUST-1; H_4BDPT = bis (3,5-dicarboxyphenyl)terephthalamide), designed from a nanosized rectangular amide-bridging tetra-carboxylate linker by solvothermal reaction of H_4BDPT and $Cu(NO_3)_2.3H_2O$ in a mixture of DMF, ethanol, and H_2O [65]. The single crystal X-ray structure reveals that the framework of HNUST-1 is constructed from paddlewheel $[Cu_2(COO)_4]$ SBUs bridged by BDPT to form a 3D non-interpenetrated (4,4)-connected net and contains two different types of the shuttle shaped and spherical pores (Fig. 5a-e) [66]. HNUST-1 exhibits a reversible type-I adsorption isotherm and takes up large amounts of N_2 at 77 K (370 cm^3 g^{-1} at 1 bar), featuring a moderate BET surface area of 1400 m^2 g^{-1}. HNUST-1 shows large CO_2-storage capacity of 53.3 wt. % at 20 bar and 273 K, as well as good selectivity of CO_2/CH_4 (7.2) and CO_2/N_2 (39.8), that is much higher than the corresponding value of MOF-177 (4.4 and 17.5) [52] and most other MOF materials [53]. Furthermore, the adsorption enthalpy of CO_2 was 31.2 kJ mol^{-1}, where a weaker CH_4 binding affinity was observed with Q_{st} of 23.4 kJ mol^{-1} (Fig. 5f). The authors attributed this behavior to be a result of the large quadrupolar moment of the CO_2 molecule which facilitates strong dipole-quadrupole interactions between the amide groups in HNUST-1 and CO_2.

In a similar study by the same group, a microporous NbO-type MOF, $[Cu_2BDPO(H_2O)_4]$ (HNUST-3), has been designed and synthesized by using a tetracarboxylate ligand of N,N′-bis(3,5-dicarboxyphenyl)oxalamide (H_4BDPO) with the "double amide" [-NHC(O)C(O)NH)-] oxalamide motif whereby two back-to-back amides comprise the bridge between two isophthalate groups [67]. The 3D framework of HNUST-3 is the first example of a porous oxalamide-functionalized MOF, made up of four connected square $[Cu_2(COO)_4]$ paddlewheels bridged through four branched BDPO linkers, while each Cu(II) center is coordinated to one water molecule along the axis of the paddlewheel. HNUST-3 exhibits a high BET surface area of 2412 m^2 g^{-1}, which is among the highest surface area of NbO-type MOF series reported to date. Moreover, HNUST-3 gives a

maximum excess H_2 uptake of 6.1 wt % (41.8 g L^{-1}) at 20 bar and 77 K which is moderate compared to the highest capacity MOF materials. Interestingly, this MOF adsorbs substantial amounts of CO_2 with uptake capacities of 33.15 wt % at 273 K and 16.6 wt % at 298 K under 1 atm of pressure, which are quite larger than that of the best performing ZIF material (ZIF-20, 13.7 wt % at 273 K and 1 atm) [68] and PCN-46 (ca. 13.2 wt % at 298 K and 1 atm) [70]. Notably, the CO_2 uptake amounts of HNUST-3 at 273 K were not saturated at 20 bar, with the values of 98.9 wt % (about 22.47 mmol g^{-1}). Interestingly, a container filled with HNUST-3 can store about 16 times the amount of CO_2 in an empty container at 20 bar and room temperature, which is higher than that for Cu-TPBTM (13 times), MOF-177 and PCN-61 (~14 times). Significantly, the strong interaction of CO_2 with the framework resulted in higher enthalpy of adsorption compared to CH_4 and N_2, leading to the high selectivity of CO_2/CH_4 (7.9) and CO_2/N_2 (26.1) at 298 K, which can be attributed to the large quadrupole moment of CO_2 as well as the presence of coordinatively unsaturated metal sites and polar oxalamide groups in HNUST-3.

In a follow-up study, Schröder and coworkers reported the uptake of CO_2 in a Cu-based porous MOF, $[Cu_2(H_2O)_2BDPO]$ (NOTT-125), using the same oxalamide H_4BDPO ligand [36]. The amide-containing linker connects $Cu_2(OOCR)$ paddle-wheels to form NOTT-125 with fof topology in which the oxalamide is incorporated and placed

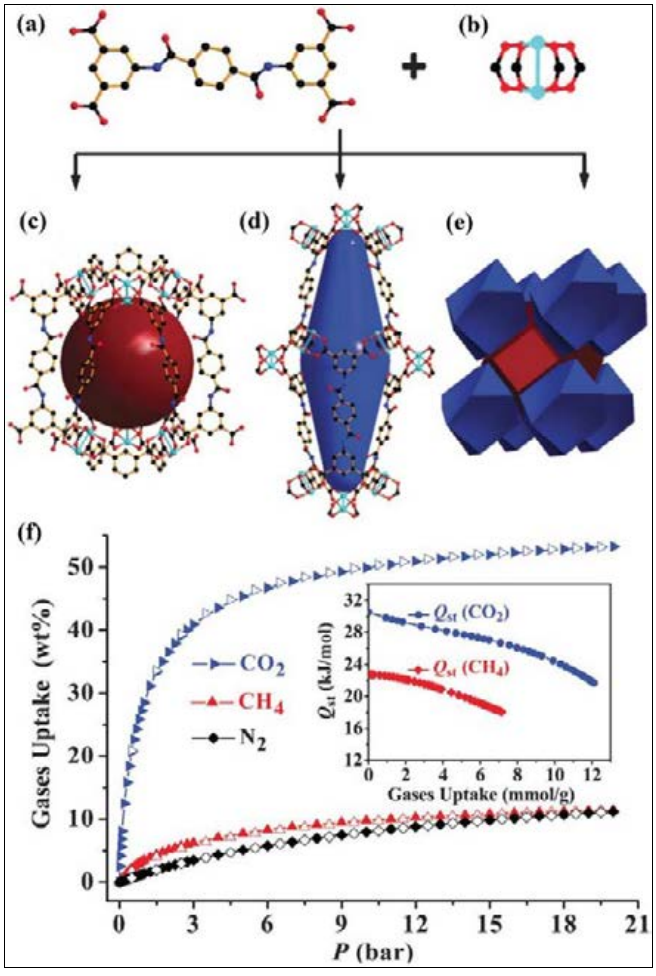

Fig. 5: (a and b) $BDPT^{4-}$ and $[Cu_2(COO)_4]$ paddlewheel cluster. (c and d) The spherical and shuttle shaped cage. (e) A natural tiling of HNUST-1. Cu, blue-green; C, black; O, red; N, blue. (b) Gas sorption properties of HNUST-1. High-pressure gravimetric excess CO_2, CH_4 and N_2 isotherms collected at 273 K (inset: isosteric heats of CO_2 and CH_4 adsorption). Filled and open symbols represent adsorption and desorption, respectively. Adapted from Ref. [65].

within the pore walls (Fig. 6a-d). The N_2 sorption isotherm for activated NOTT-125 at 77 K exhibits reversible type I adsorption behavior with the BET surface area of 2447 m^2 g^{-1}. The oxalamide groups in the pore walls, combined with the large pore volume of this MOF has afforded the enhanced CO_2 uptake of 40.1 wt % at 273 K and 1 bar, which approaches the highest reported values for MOFs, such as Cu-TDPAT (44.5 wt%) [70] and Cu-TPBTM (42.6 wt%) [37], and is higher than the related amide-functionalized MOFs of Cu-NJU-Bai3 and PCN-124 (Fig. 6e,f). Moreover, its high pressure CO_2 uptake (21.2 mmol g^{-1} at 298 K and 20 bar) and adsorption enthalpy (25.35 kJ mol^{-1}) could be attributed to the specific CO_2-oxamide interactions, including dipole-quadrupole interactions and hydrogen-bond formation between the amide NH and the oxygen atoms of CO_2, which further verified by GCMC simulations.

Advances in the field of porous solids have been recently realized through the development of MOFs that are flexible. These so-called "third generation materials" are unique in their ability to undergo structural changes during the adsorption and desorption of guests, inducing highly-selective guest accommodation and magnetic modulation [71, 72]. The first gate-opening behavior of amide-functionalized MOF has been reported by Ghosh and co-workers, where the amide integrated framework of $[CuL_2(NO_3)_2 \cdot o\text{-xylene} \cdot DMF]_n$ (1-NO_3^-), based on a flexible neutral amide-based N-donor ligand, was discriminated between CO_2

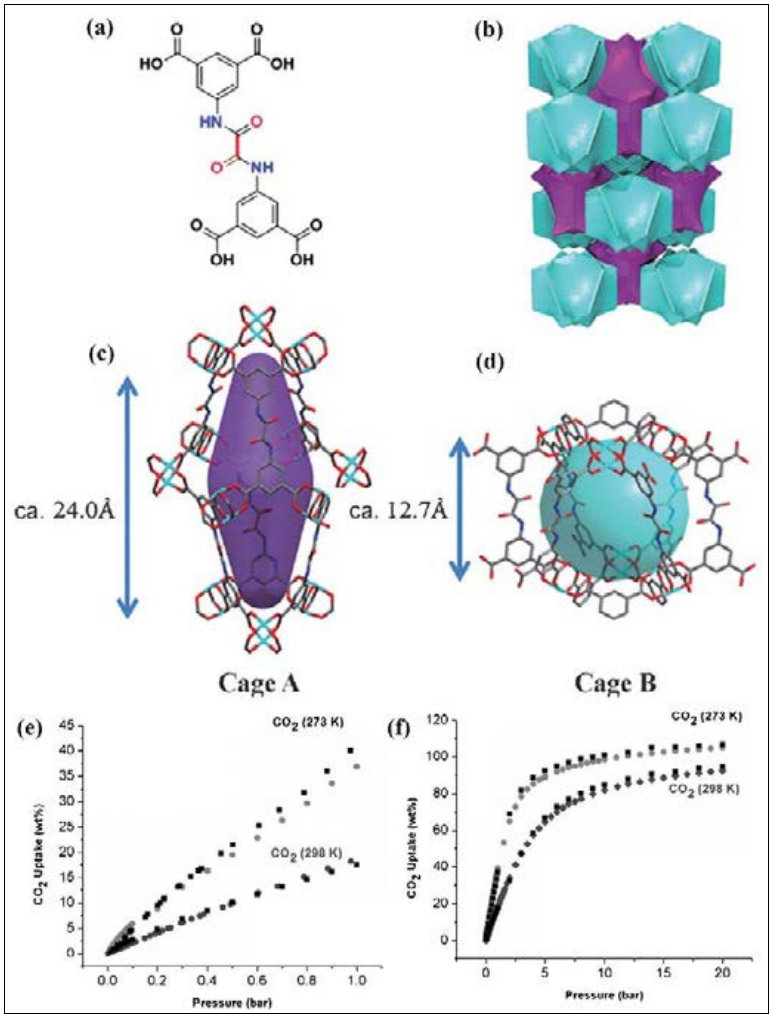

Fig. 6: View of: (a) Chemical structure of H_4BDPO; (b) Tiling of NOTT-125; (c) Cage A, and (d) Cage B. Experimental (circles) and simulated (squares) CO_2 isotherms of NOTT-125 at 273 and 298 K in the pressure range (e) 0-1 and (f) up to 20 bar. Adapted from Ref. [36].

as a polar gas molecule and other nonpolar gases [73] (Fig. 7a,b). Upon desolvation, this compound undergoes a dynamic structural transformation from a 1D porous phase to a 2D non-porous phase. Interestingly, 1-NO_3^- showed a CO_2 uptake of around 84 cm^3 g^{-1}, whereas the compound shows a negligible uptake for other gases (N_2, H_2, Ar, and CH_4) (Fig. 7c). Such selectivity of CO_2 and corresponding transformation from the nonporous phase to microporous phase can be ascribed to the strong dipole-quadrupolar interaction of the -CONH- groups with the incoming CO_2 molecules.

In a similar study, the amide-CO_2 interaction was induced gate-opening behavior for CO_2 adsorption in flexible 2-fold interpenetrating network of $[Mn_2(2,6\text{-ndc})_2(bpda)_2]\cdot 5DMF$ (Mn-bpda) with amide groups exposed in the channels [74]. The N_2 adsorption isotherms of MOF showed only a minor uptake at 77 K, which can be attributed to framework contraction and a lack of appropriate intermolecular interactions at low temperature, where the adsorption isotherms for CO_2 at 195 K displayed a gate-opening adsorption, with a total amount of CO_2 adsorption of 143 cm^3 g^{-1}, and a corresponding isosteric heat of adsorption of 26.9 kJ mol^{-1} which increases to 36.2 kJ mol^{-1} with increasing CO_2 uptake. Moreover, the high pressure CO_2 adsorption isotherm of the flexible species Mn-bpda indicated a marked gate-opening process at P=5-8 bar, which was not found for N_2 adsorption (Fig. 8). These results show that amide-CO_2 interactions and possible amide-CO_2-CO_2 interactions play important roles in causing structural variations and in inducing the gate-opening behavior for CO_2 adsorption [75].

Recently, a pillaring strategy has been used for the design and synthesis of three interpenetrated amide-functionalized MOFs, TMUs-22/-23/-24, with the V-shaped dicarboxylate ligand of 4,4'-oxybisbenzoic acid (H_2oba) and linear

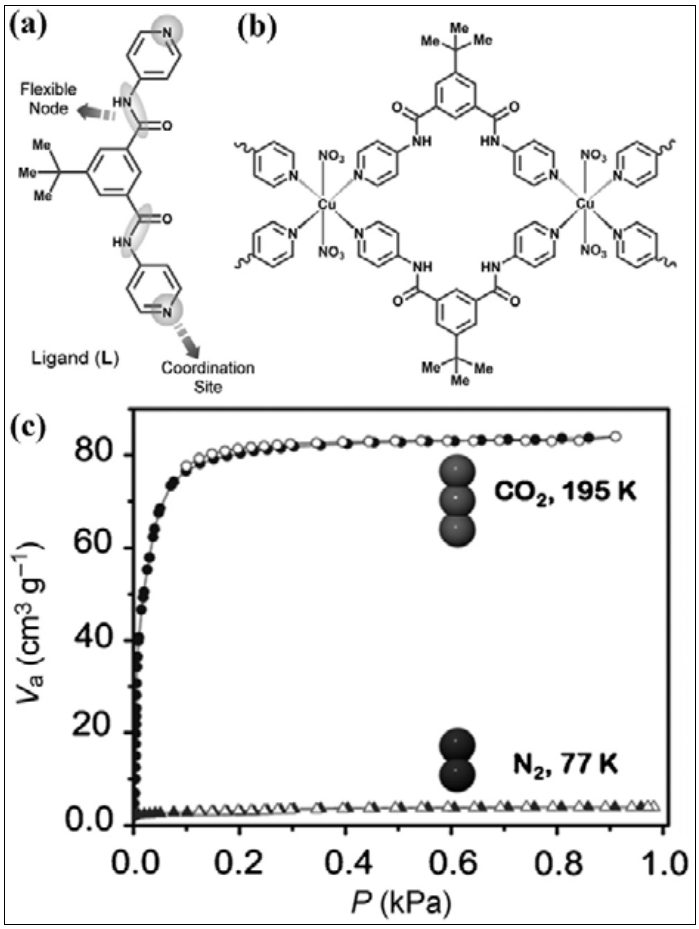

Fig. 7: (a) The ligand L and (b) the coordination environment around the copper center in 1-NO_3^-. (b) CO_2 and N_2 adsorption isotherm at 195 K and 77 K respectively showing separation. Adapted from Ref. [73].

dipyridyl-based ligands, which are isoreticular to the imine-functionalized TMUs-6/-21 MOFs [76] (Fig. 9a). The similarities (structure and stability) and differences (functional group and accessibility) of these MOFs allow study of the influence of the amide and the imine groups on their N_2 and CO_2 sorption properties as well as on their selective sorption of CO_2 over N_2. Interestingly, extensive study of their CO_2 sorption properties and selectivity, evaluated by performing kinetics

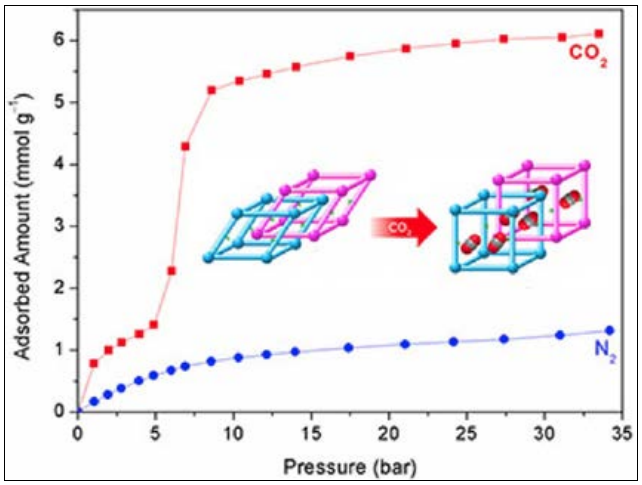

Fig. 8: Amide-CO_2 interactions induced gate-opening behavior for CO_2 adsorption at 298 K. Adapted from Ref. [74].

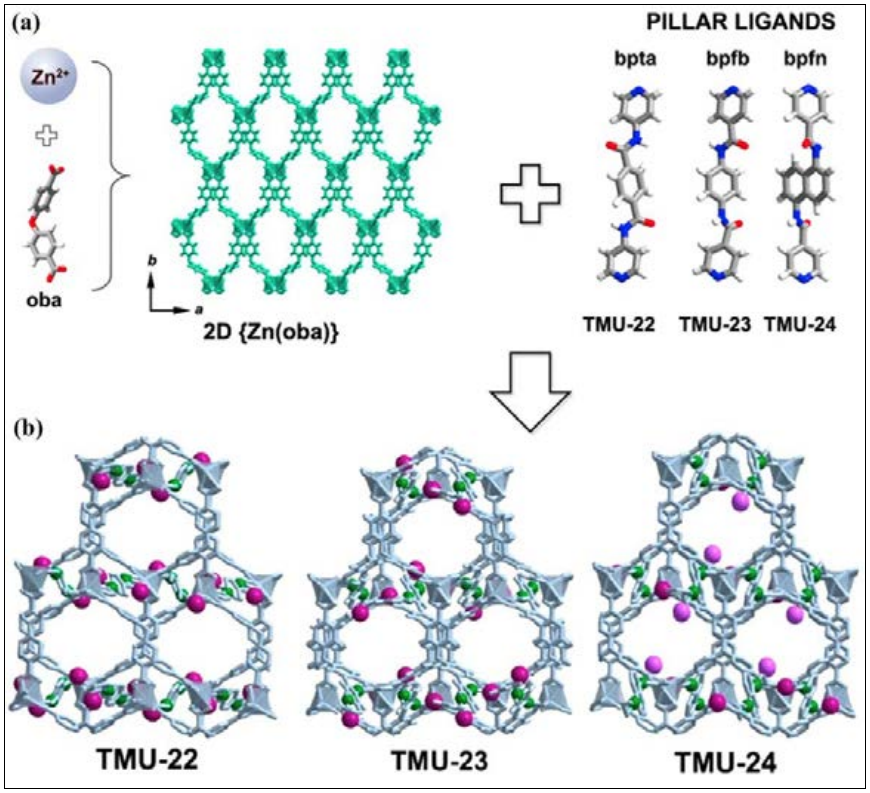

Fig. 9: (a) 2D layers formed by the association between Zn(II) ions and oba linkers are further pillared by amide/imine-functionalized dipyridyl-based ligands yielding to threefold interpenetrated porous pcu-MOFs. (b) View of the pore channels of TMUs-22/-23/-24, highlighting the amide groups. Color code: N (green), O (purple), the more accessible O atoms in TMU-24 (lavender). Adapted from Ref. [76].

and breakthrough experiments for a CO_2/N_2 gas mixture, revealed that not only the incorporation of amide groups but also their accessibility is crucial to obtain enhanced CO_2 sorption and CO_2/N_2 selectivity (Fig. 9b). Therefore, the MOF with more accessible amide groups (TMU-24) shows a CO_2/N_2 selectivity value of ca. 10 (as revealed by breakthrough experiments), which is ca. 500% and 700% of the selectivity values observed for the other amide-containing (TMUs-22/-23) and imine-containing (TMUs-6/-21) MOFs, respectively.

MOFs are amenable to various post-synthesis manipulations to incorporate desired chemical moieties into nanoscale pores. In a valuable work performed by Hupp and Farha, two complementary amide-containing organic motifs (Fig. 10 a,b), which have a partial charges ($\delta^+\ldots\delta^-\ldots\delta^+$) precisely positioned via polar organic functionalities to complement the quadrupolar charge distribution in O=C=O, were post-synthetically incorporated into the robust NU-1000 MOF using solvent-assisted ligand incorporation (SALI) for CO_2 capture and separation [77] (Fig. 10c-e). Previous studies have established that SALI relies on Zr(IV)-carboxylate bond formation on the NU-1000 node to incorporate chemical moieties, provides a platform to evaluate the performance of new chemical functionalities in a porous solid environment without the need to prepare a new MOF linker containing the chemical functionality of interest, and enhances chemical and water vapor stability [77, 78]. Both of the amide-decorated SALI-derived samples entailed a slightly steeper CO_2 uptake in the CO_2 adsorption profiles at low

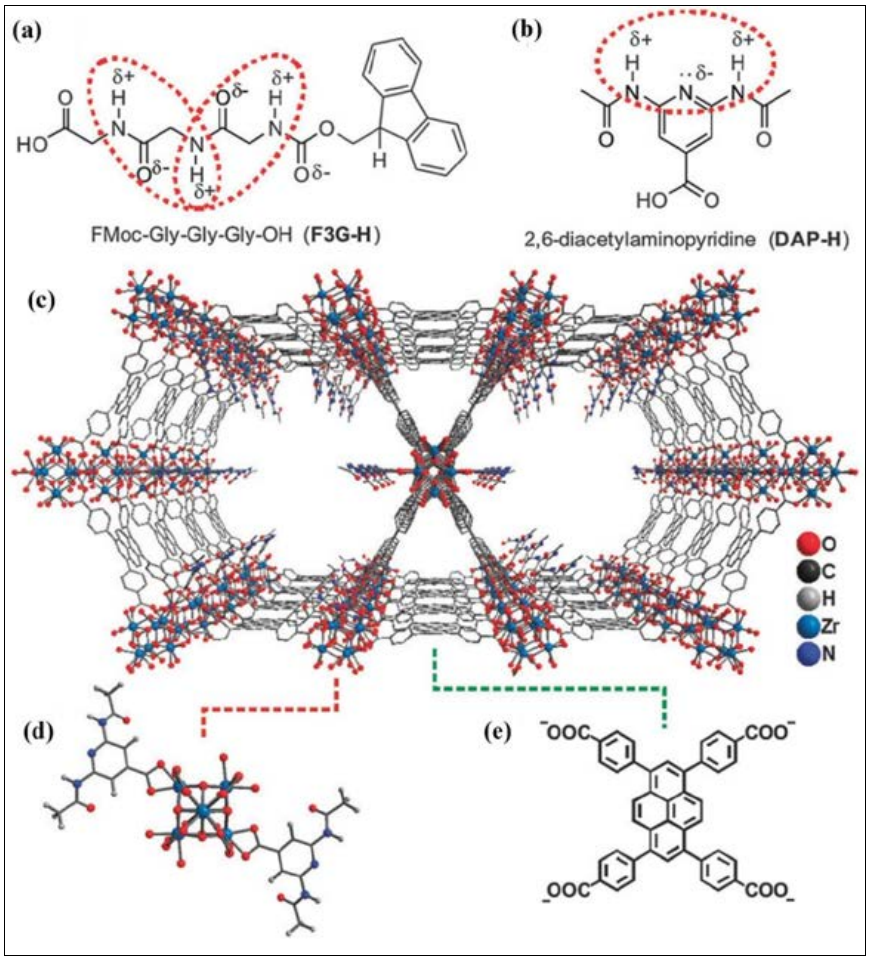

Fig. 10: Schematic representations of (a) N-α-fluorenylmethyloxycarbonyl protected triglycine and (b) 2,6-diacetylaminopyridine-4-carboxylic acid. SALI, a heterogenization strategy for carboxylic acid-derived functional groups, applied to the MOF NU-1000: (c) molecular representation of SALI-derived SALI-DAP (along the c-axis), (d) the corresponding functionalized node, and (d) the linker of NU-1000. Adapted from Ref. [77].

pressure, resulting in higher volumetric uptake at lower pressure (~0.2 bar) relative to the unmodified NU-1000. Moreover, the post-modified samples showed higher values for Q_{st} at the zero-loading limit (27-28 kJ mol^{-1}) than the parent NU-1000 (17 kJ mol^{-1}), as qualitatively predicted by the GCMC simulations.

Very recently, an exceptionally water stable highly porous 3D MOF, $[Cu_2(PDAD)(H_2O)]_n$ (PCN-124-stu, H_4PDAD = 5,5′-(pyridine-3,5-dicarbonyl)bis(azanediyl)diisophthalic acid), has been synthesized with amide-functionalized cages [79]. PCN-124-stu maintains its framework in water with different pH values (pH 2-12) for at least one week, as monitored by PXRD, while only a limited number of MOFs have excellent stability in such a wide pH range of aqueous solutions, including those constructed MOFs with relatively expensive metals such as Zr which have higher metal-oxygen coordination bond energies. Compared to prototypical MOF PCN-124, PCN-124-stu exhibits larger pore sizes, higher porosity, and larger surface area. However, compared to the CO_2 capacities of PCN-124 under the same conditions, those of MOFs PCN-124-stu are reduced to some extent, which this may be attributable to the larger surface area and porosity of the latter. Through GCMC simulation at 273 K and 1 bar, the zero-loading heats of adsorption were found to be 26 kJ mol^{-1} for CO_2 and 15 kJ mol^{-1} for CH_4, which show significant selective adsorption of CO_2 over CH_4. Furthermore, the GCMC simulations revealed that both open Cu^{II} metal sites and the amide groups in the framework are clearly the main adsorption sites of CO_2 molecules, where H-bonding and van der Waals forces are the main interactions between CO_2 molecules and amide groups in the lowest-energy framework.

In 2016, Schröder and coworkers reported an amide-functionalized pyrimidyl Cu(II)-carboxylate MOF, MFM-136, which shows a CO_2 uptake of 14.3 mmol g^{-1} at 20 bar and 273 K, representing the highest CO_2 uptake in mono-amide-functionalized MOFs reported to date [80]. In contrast, MFM-136 gives a lower uptake of CH_4 (8.3 mmol g^{-1}) and negligible uptake of N_2 under the same conditions, leading to selectivities of 6.3:1 and 27:1 for CO_2/CH_4 and CO_2/N_2, respectively. In this MOF, all Cu(II) sites are fully coordinated to carboxylate and pyrimidyl groups, affording a pore environment without open metal sites, which provides an ideal environment for studying the binding interaction between amides and adsorbed CO_2 molecules, since it eliminates the competitive binding of CO_2 on the open Cu(II) sites. It is noteworthy that despite the good CO_2 uptake properties of MFM-136, combined neutron diffraction and inelastic neutron spectroscopy indicate no direct binding between adsorbed CO_2/CH_4 and free amides in this case. This suggests that introduction of functional groups solely may not necessarily induce specific guest-host binding in the porous material, but it is a combination of pore size, geometry, and functional group that leads to enhanced gas adsorption properties. However, for further comparison it would be well to perform the CO_2 uptake of the isostructural MOF, which has the same pore size and geometry as MFM-136 but without amide functional groups inside the pores.

CONCLUSIONS AND PERSPECTIVES

Currently, there is no unique solution to solve the problem of CO_2 capture, and this complicated challenge will almost certainly require the integration of several technology options. This review article has sought to highlight the effects of amide groups in the pores of MOFs on the CO_2 storage and separation abilities, which are dramatically enhanced by generation of specific metal-free polar functional groups within the porous MOFs because the functional moieties directly recognize CO_2 molecules through strong interactions. Furthermore, in parallel with experimental studies, in some cases, computational modeling methods such as grand canonical Monte Carlo (GCMC) and first-principles calculations have been applied as a tool to further probe the advantages of amide groups upon CO_2 adsorption at the molecular level, which demonstrated that CO_2 molecules prefer to locate at amide groups within the frameworks. Finally, we anticipate that this review article can provide useful information on the significant progress of the enhancement of CO_2 capture by decorating amide functional groups within the pores of MOF materials, which is very promising for real-world applications where MOF materials could be capable of serving as next-generation CO_2 capture systems.

ACKNOWLEDGEMENT

The financial support of this investigation by Iran University of Science and Technology is gratefully acknowledged.

CONFLICT OF INTEREST

The authors declare that there is no conflict of interests regarding the publication of this paper.

ABBREVIATIONS

BDC = 1,4-benzyldicarboxylate

bipy = 4,4′-bipyridine

bpe = 1,2-bis(4-pyridyl)-ethene

bpda = N,N′-bis(4-pyridinyl)-1,4-benzene dicarboxamide

bpfb = N,N′-bis-(4-pyridylformamide)-1,4-benzenediamine

bpfn = N,N′-bis(4-pyridylformamide)-1,5-naphthalenediamine

bpta = N,N′-bis(4-pyridinyl)terephthalamide

bpp = 1,3-bis(4-pyridyl)propane

$btei^{6-}$ = 5,5′,5″-benzene-1,3,5-triyltris(1-ethynyl-2-isophthalate)

CCS = Carbon capture and sequestration

H_3L = (5-(4-carboxybenzoylamino)-isophthalic acid)

H_4BDPT = bis(3,5-dicarboxyphenyl)terephthalamide

H_4BDPO = N,N′-bis(3,5 dicarboxyphenyl)oxalamide

H_4PDAD = 5,5′-(pyridine-3,5-dicarbonyl) bis(azanediyl)diisophthalic acid

H_6BTB = 5,5’,5”-((5’-(4-formylphenyl)-[1,1’:3’,1”-terphenyl]-4,4”-dicarbonyl)tris(azanediyl)) triisophthalic acid

H_6TATB=5,5’,5”-((4,4’,4”-(1,3,5-triazine-2,4,6-triyl) tris(benzoyl))tris(azanediyl))triisophthalic acid

GCMC = Grand canonical Monte Carlo

MOFs = Metal-organic frameworks

2,6-ndc=2,6-naphthalene dicarboxylate

PDAI = 5,5′-((pyridine-3,5-dicarbonyl)bis-(azanediyl)) diisophthalate

pia = N-(pyridin-4-yl)isonicotinamide

TBAPy = 1,3,6,8-tetrakis(p-benzoic acid)pyrene

TPBTM = N,N’,N”-tris(isophthalyl)-1,3,5-benzenetricarboxamide

TCMBT = N,N′,N″-tris(carboxymethyl)-1,3,5-benzenetricarboxamide

REFERENCES

1. Song C. Global challenges and strategies for control, conversion and utilization of CO2 for sustainable development involving energy, catalysis, adsorption and chemical processing. Catalysis Today. 2006;115(1):2-32.
2. Yu KMK, Curcic I, Gabriel J, Tsang SCE. Recent Advances in CO2Capture and Utilization. ChemSusChem. 2008;1(11):893-9.
3. Sakakura T, Choi J-C, Yasuda H. Transformation of Carbon Dioxide. Chemical Reviews. 2007;107(6):2365-87.
4. Suh MP, Park HJ, Prasad TK, Lim D-W. Hydrogen Storage in Metal–Organic Frameworks. Chemical Reviews. 2012;112(2):782-835.
5. Liu J, Thallapally PK, McGrail BP, Brown DR, Liu J. Progress in adsorption-based CO2 capture by metal-organic frameworks. Chemical Society Reviews. 2012;41(6):2308-22.
6. Sumida K, Rogow DL, Mason JA, McDonald TM, Bloch ED, Herm ZR, et al. Carbon Dioxide Capture in Metal–Organic Frameworks. Chemical Reviews. 2012;112(2):724-81.
7. Zhang Z, Zhao Y, Gong Q, Li Z, Li J. MOFs for CO2 capture and separation from flue gas mixtures: the effect of multifunctional sites on their adsorption capacity and selectivity. Chemical Communications. 2013;49(7):653-61.
8. Li J-R, Sculley J, Zhou H-C. Metal–Organic Frameworks for Separations. Chemical Reviews. 2012;112(2):869-932.
9. Han D, Jiang F-L, Wu M-Y, Chen L, Chen Q-H, Hong M-C. A non-interpenetrated porous metal-organic framework with high gas-uptake capacity. Chemical Communications. 2011;47(35):9861-3.
10. Safarifard V, Morsali A. Facile preparation of nanocubes zinc-based metal-organic framework by an ultrasound-assisted synthesis method; precursor for the fabrication of zinc oxide octahedral nanostructures. Ultrasonics Sonochemistry. 2018;40:921-8.
11. Zhou H-C, Long JR, Yaghi OM. Introduction to Metal–Organic Frameworks. Chemical Reviews. 2012;112(2):673-4.
12. Millward AR, Yaghi OM. Metal–Organic Frameworks with Exceptionally High Capacity for Storage of Carbon Dioxide at Room Temperature. Journal of the American Chemical Society. 2005;127(51):17998-9.
13. Llewellyn PL, Bourrelly S, Serre C, Vimont A, Daturi M, Hamon L, et al. High Uptakes of CO2 and CH4 in Mesoporous Metal—Organic Frameworks MIL-100 and MIL-101. Langmuir. 2008;24(14):7245-50.
14. Yuan D, Zhao D, Sun D, Zhou HC. An Isoreticular Series of Metal–Organic Frameworks with Dendritic Hexacarboxylate Ligands and Exceptionally High Gas-Uptake Capacity. Angewandte Chemie International Edition. 2010;49(31):5357-61.
15. Furukawa H, Ko N, Go YB, Aratani N, Choi SB, Choi E, et al. Ultrahigh Porosity in Metal-Organic Frameworks. Science. 2010;329(5990):424-8.
16. Debatin F, Thomas A, Kelling A, Hedin N, Bacsik Z, Senkovska I, et al. In Situ Synthesis of an Imidazolate-4-amide-5-imidate Ligand and Formation of a Microporous Zinc-Organic Framework with H2-and CO2-Storage Ability. Angewandte Chemie International Edition. 2010;49(7):1258-62.
17. An J, Geib SJ, Rosi NL. High and Selective CO2Uptake in a Cobalt Adeninate Metal–Organic Framework Exhibiting Pyrimidine- and Amino-Decorated Pores. Journal of the American Chemical Society. 2010;132(1):38-9.
18. Vaidhyanathan R, Iremonger SS, Dawson KW, Shimizu GKH. An amine-functionalized metal organic framework for preferential CO2 adsorption at low pressures. Chemical Communications. 2009(35):5230.

19. Arstad B, Fjellvåg H, Kongshaug KO, Swang O, Blom R. Amine functionalised metal organic frameworks (MOFs) as adsorbents for carbon dioxide. Adsorption. 2008;14(6):755-62.
20. Couck S, Denayer JFM, Baron GV, Rémy T, Gascon J, Kapteijn F. An Amine-Functionalized MIL-53 Metal–Organic Framework with Large Separation Power for CO2and CH4. Journal of the American Chemical Society. 2009;131(18):6326-7.
21. Lin J-B, Zhang J-P, Chen X-M. Nonclassical Active Site for Enhanced Gas Sorption in Porous Coordination Polymer. Journal of the American Chemical Society. 2010;132(19):6654-6.
22. Torrisi A, Bell RG, Mellot-Draznieks C. Functionalized MOFs for Enhanced CO2Capture. Crystal Growth & Design. 2010;10(7):2839-41.
23. Liu B, Yang Q, Xue C, Zhong C, Chen B, Smit B. Enhanced Adsorption Selectivity of Hydrogen/Methane Mixtures in Metal–Organic Frameworks with Interpenetration: A Molecular Simulation Study. The Journal of Physical Chemistry C. 2008;112(26):9854-60.
24. Cheon YE, Park J, Suh MP. Selective gas adsorption in a magnesium-based metal–organic framework. Chemical Communications. 2009(36):5436.
25. Kim J, Yang S-T, Choi SB, Sim J, Kim J, Ahn W-S. Control of catenation in CuTATB-n metal–organic frameworks by sonochemical synthesis and its effect on CO2 adsorption. Journal of Materials Chemistry. 2011;21(9):3070.
26. Britt D, Furukawa H, Wang B, Glover TG, Yaghi OM. Highly efficient separation of carbon dioxide by a metal-organic framework replete with open metal sites. Proceedings of the National Academy of Sciences. 2009;106(49):20637-40.
27. Demessence A, D'Alessandro DM, Foo ML, Long JR. Strong CO2Binding in a Water-Stable, Triazolate-Bridged Metal–Organic Framework Functionalized with Ethylenediamine. Journal of the American Chemical Society. 2009;131(25):8784-6.
28. Yazaydın AOzr, Benin AI, Faheem SA, Jakubczak P, Low JJ, Willis RR, et al. Enhanced CO2Adsorption in Metal-Organic Frameworks via Occupation of Open-Metal Sites by Coordinated Water Molecules. Chemistry of Materials. 2009;21(8):1425-30.
29. Prasad TK, Hong DH, Suh MP. High Gas Sorption and Metal-Ion Exchange of Microporous Metal-Organic Frameworks with Incorporated Imide Groups. Chemistry - A European Journal. 2010;16(47):14043-50.
30. Banerjee R, Furukawa H, Britt D, Knobler C, O'Keeffe M, Yaghi OM. Control of Pore Size and Functionality in Isoreticular Zeolitic Imidazolate Frameworks and their Carbon Dioxide Selective Capture Properties. Journal of the American Chemical Society. 2009;131(11):3875-7.
31. Deng H, Doonan CJ, Furukawa H, Ferreira RB, Towne J, Knobler CB, et al. Multiple Functional Groups of Varying Ratios in Metal-Organic Frameworks. Science. 2010;327(5967):846-50.
32. Zhao X, Sun D, Yuan S, Feng S, Cao R, Yuan D, et al. Comparison of the Effect of Functional Groups on Gas-Uptake Capacities by Fixing the Volumes of Cages A and B and Modifying the Inner Wall of Cage C in rht-Type MOFs. Inorganic Chemistry. 2012;51(19):10350-5.
33. Si X, Jiao C, Li F, Zhang J, Wang S, Liu S, et al. High and selective CO2 uptake, H2 storage and methanol sensing on the amine-decorated 12-connected MOF CAU-1. Energy & Environmental Science. 2011;4(11):4522.
34. Tanhaei M, Mahjoub AR, Safarifard V. Sonochemical synthesis of amide-functionalized metal-organic framework/graphene oxide nanocomposite for the adsorption of methylene blue from aqueous solution. Ultrasonics Sonochemistry. 2018;41:189-95.
35. Du L, Yang S, Xu L, Min H, Zheng B. Highly selective carbon dioxide uptake by a microporous kgm-pillared metal–organic framework with acylamide groups. CrystEngComm. 2014;16(25):5520.
36. Alsmail NH, Suyetin M, Yan Y, Cabot R, Krap CP, Lü J, et al. Analysis of High and Selective Uptake of CO2in an Oxamide-Containing {Cu2(OOCR)4}-Based Metal-Organic Framework. Chemistry - A European Journal. 2014;20(24):7317-24.
37. Zheng B, Bai J, Duan J, Wojtas L, Zaworotko MJ. Enhanced CO2Binding Affinity of a High-Uptakerht-Type Metal–Organic Framework Decorated with Acylamide Groups. Journal of the American Chemical Society. 2011;133(4):748-51.
38. Chen Y-Q, Qu Y-K, Li G-R, Zhuang Z-Z, Chang Z, Hu T-L, et al. Zn(II)-Benzotriazolate Clusters Based Amide Functionalized Porous Coordination Polymers with High CO2 Adsorption Selectivity. Inorganic Chemistry. 2014;53(17):8842-4.
39. Chen Z, Adil K, Weseliński ŁJ, Belmabkhout Y, Eddaoudi M. A supermolecular building layer approach for gas separation and storage applications: the eea and rtl MOF platforms for CO2 capture and hydrocarbon separation. Journal of Materials Chemistry A. 2015;3(12):6276-81.
40. Lu Z, Bai J, Hang C, Meng F, Liu W, Pan Y, et al. The Utilization of Amide Groups To Expand and Functionalize Metal-Organic Frameworks Simultaneously. Chemistry - A European Journal. 2016;22(18):6277-85.
41. Gharib M, Safarifard V, Morsali A. Ultrasound assisted synthesis of amide functionalized metal-organic framework for nitroaromatic sensing. Ultrasonics Sonochemistry. 2018;42:112-8.
42. Xiong S, He Y, Krishna R, Chen B, Wang Z. Metal–Organic Framework with Functional Amide Groups for Highly Selective Gas Separation. Crystal Growth & Design. 2013;13(6):2670-4.
43. Trickett CA, Helal A, Al-Maythalony BA, Yamani ZH, Cordova KE, Yaghi OM. The chemistry of metal–organic frameworks for CO 2 capture, regeneration and conversion. Nature Reviews Materials. 2017;2(8):17045.
44. Pera-Titus M. Porous Inorganic Membranes for CO2 Capture: Present and Prospects. Chemical Reviews. 2013;114(2):1413-92.
45. Belmabkhout Y, Guillerm V, Eddaoudi M. Low concentration CO 2 capture using physical adsorbents: Are metal–organic frameworks becoming the new benchmark materials?

Chemical Engineering Journal. 2016;296:386-97.
46. González-Zamora E, Ibarra IA. CO2 capture under humid conditions in metal–organic frameworks. Materials Chemistry Frontiers. 2017;1(8):1471-84.
47. Nouar F, Eubank JF, Bousquet T, Wojtas L, Zaworotko MJ, Eddaoudi M. Supermolecular Building Blocks (SBBs) for the Design and Synthesis of Highly Porous Metal-Organic Frameworks. Journal of the American Chemical Society. 2008;130(6):1833-5.
48. Zhao D, Yuan D, Sun D, Zhou H-C. Stabilization of Metal–Organic Frameworks with High Surface Areas by the Incorporation of Mesocavities with Microwindows. Journal of the American Chemical Society. 2009;131(26):9186-8.
49. Yan Y, Lin X, Yang S, Blake AJ, Dailly A, Champness NR, et al. Exceptionally high H2 storage by a metal–organic polyhedral framework. Chemical Communications. 2009(9):1025.
50. Zheng B, Yang Z, Bai J, Li Y, Li S. High and selective CO2 capture by two mesoporous acylamide-functionalized rht-type metal–organic frameworks. Chemical Communications. 2012;48(56):7025.
51. Farha OK, Özgür Yazaydın A, Eryazici I, Malliakas CD, Hauser BG, Kanatzidis MG, et al. De novo synthesis of a metal–organic framework material featuring ultrahigh surface area and gas storage capacities. Nature Chemistry. 2010;2(11):944-8.
52. Saha D, Bao Z, Jia F, Deng S. Adsorption of CO2, CH4, N2O, and N2on MOF-5, MOF-177, and Zeolite 5A. Environmental Science & Technology. 2010;44(5):1820-6.
53. Li J-R, Ma Y, McCarthy MC, Sculley J, Yu J, Jeong H-K, et al. Carbon dioxide capture-related gas adsorption and separation in metal-organic frameworks. Coordination Chemistry Reviews. 2011;255(15-16):1791-823.
54. Vogiatzis KD, Mavrandonakis A, Klopper W, Froudakis GE. Ab initio Study of the Interactions between CO2and N-Containing Organic Heterocycles. ChemPhysChem. 2009;10(2):374-83.
55. Duan J, Yang Z, Bai J, Zheng B, Li Y, Li S. Highly selective CO2 capture of an agw-type metal–organic framework with inserted amides: experimental and theoretical studies. Chemical Communications. 2012;48(25):3058.
56. Wong-Foy AG, Lebel O, Matzger AJ. Porous Crystal Derived from a Tricarboxylate Linker with Two Distinct Binding Motifs. Journal of the American Chemical Society. 2007;129(51):15740-1.
57. Kim H, Kim Y, Yoon M, Lim S, Park SM, Seo G, et al. Highly Selective Carbon Dioxide Sorption in an Organic Molecular Porous Material. Journal of the American Chemical Society. 2010;132(35):12200-2.
58. Bae Y-S, Spokoyny AM, Farha OK, Snurr RQ, Hupp JT, Mirkin CA. Separation of gas mixtures using Co(ii) carborane-based porous coordination polymers. Chemical Communications. 2010;46(20):3478.
59. Park J, Li J-R, Chen Y-P, Yu J, Yakovenko AA, Wang ZU, et al. A versatile metal–organic framework for carbon dioxide capture and cooperative catalysis. Chemical Communications. 2012;48(80):9995.
60. Burd SD, Ma S, Perman JA, Sikora BJ, Snurr RQ, Thallapally PK, et al. Highly Selective Carbon Dioxide Uptake by [Cu(bpy-n)2(SiF6)] (bpy-1 = 4,4′-Bipyridine; bpy-2 = 1,2-Bis(4-pyridyl)ethene). Journal of the American Chemical Society. 2012;134(8):3663-6.
61. Lee C-H, Huang H-Y, Liu Y-H, Luo T-T, Lee G-H, Peng S-M, et al. Cooperative Effect of Unsheltered Amide Groups on CO2 Adsorption Inside Open-Ended Channels of a Zinc(II)–Organic Framework. Inorganic Chemistry. 2013;52(7):3962-8.
62. Lu Z, Xing H, Sun R, Bai J, Zheng B, Li Y. Water Stable Metal–Organic Framework Evolutionally Formed from a Flexible Multidentate Ligand with Acylamide Groups for Selective CO2 Adsorption. Crystal Growth & Design. 2012;12(3):1081-4.
63. Wang B, Côté AP, Furukawa H, O'Keeffe M, Yaghi OM. Colossal cages in zeolitic imidazolate frameworks as selective carbon dioxide reservoirs. Nature. 2008;453(7192):207-11.
64. Bae YS, Lee CH. Sorption kinetics of eight gases on a carbon molecular sieve at elevated pressure. Carbon. 2005;43(1):95-107.
65. Zheng B, Liu H, Wang Z, Yu X, Yi P, Bai J. Porous NbO-type metal–organic framework with inserted acylamide groups exhibiting highly selective CO2 capture. CrystEngComm. 2013;15(18):3517.
66. Chen B, Ockwig NW, Millward AR, Contreras DS, Yaghi OM. High H2 Adsorption in a Microporous Metal-Organic Framework with Open Metal Sites. Angewandte Chemie International Edition. 2005;44(30):4745-9.
67. Wang Z, Zheng B, Liu H, Lin X, Yu X, Yi P, et al. High-Capacity Gas Storage by a Microporous Oxalamide-Functionalized NbO-Type Metal–Organic Framework. Crystal Growth & Design. 2013;13(11):5001-6.
68. Phan A, Doonan CJ, Uribe-Romo FJ, Knobler CB, O'Keeffe M, Yaghi OM. Synthesis, Structure, and Carbon Dioxide Capture Properties of Zeolitic Imidazolate Frameworks. Accounts of Chemical Research. 2010;43(1):58-67.
69. Wang X-F, Zhang Y-B, Zhang W-X, Xue W, Zhou H-L, Chen X-M. Buffering additive effect in the formation of metal–carboxylate frameworks with slightly different linear M3(RCOO)6 clusters. CrystEngComm. 2011;13(12):4196.
70. Li B, Zhang Z, Li Y, Yao K, Zhu Y, Deng Z, et al. Enhanced Binding Affinity, Remarkable Selectivity, and High Capacity of CO2 by Dual Functionalization of a rht-Type Metal-Organic Framework. Angewandte Chemie International Edition. 2011;51(6):1412-5.
71. Li C-P, Chen J, Liu C-S, Du M. Dynamic structural transformations of coordination supramolecular systems upon exogenous stimulation. Chemical Communications. 2015;51(14):2768-81.
72. Kitagawa S, Uemura K. Dynamic porous properties of coordination polymers inspired by hydrogen bonds. Chemical Society Reviews. 2005;34(2):109.
73. Karmakar A, Desai AV, Manna B, Joarder B, Ghosh SK. An Amide-Functionalized Dynamic Metal–Organic Framework Exhibiting Visual Colorimetric Anion Exchange and Selective Uptake of Benzene over Cyclohexane.

Chemistry-A European Journal. 2015;21(19):7071-6.
74. Lee C-H, Huang H-Y, Lee J-J, Huang C-Y, Kao Y-C, Lee G-H, et al. Amide-CO2Interaction Induced Gate-Opening Behavior for CO2Adsorption in 2-Fold Interpenetrating Framework. ChemistrySelect. 2016;1(11):2923-9.
75. Choi H-S, Suh MP. Highly Selective CO2Capture in Flexible 3D Coordination Polymer Networks. Angewandte Chemie International Edition. 2009;48(37):6865-9.
76. Safarifard V, Rodríguez-Hermida S, Guillerm V, Imaz I, Bigdeli M, Azhdari Tehrani A, et al. Influence of the Amide Groups in the CO2/N2 Selectivity of a Series of Isoreticular, Interpenetrated Metal–Organic Frameworks. Crystal Growth & Design. 2016;16(10):6016-23.
77. Deria P, Li S, Zhang H, Snurr RQ, Hupp JT, Farha OK. A MOF platform for incorporation of complementary organic motifs for CO_2 binding. Chemical Communications. 2015;51(62):12478-81.
78. Deria P, Bury W, Hod I, Kung C-W, Karagiaridi O, Hupp JT, et al. MOF Functionalization via Solvent-Assisted Ligand Incorporation: Phosphonates vs Carboxylates. Inorganic Chemistry. 2015;54(5):2185-92.
79. Jin W-G, Chen W, Xu P-H, Lin X-W, Huang X-C, Chen G-H, et al. An Exceptionally Water Stable Metal-Organic Framework with Amide-Functionalized Cages: Selective CO2 /CH4 Uptake and Removal of Antibiotics and Dyes from Water. Chemistry - A European Journal. 2017;23(53):13058-66.
80. Benson O, da Silva I, Argent SP, Cabot R, Savage M, Godfrey HGW, et al. Amides Do Not Always Work: Observation of Guest Binding in an Amide-Functionalized Porous Metal–Organic Framework. Journal of the American Chemical Society. 2016;138(45):14828-31.